

Torsional selection rule for the spin–orbit conversion of light

Edilberto O. Silva^{1,*}

¹*Programa de Pós-Graduação em Física & Coordenação do Curso de Física – Bacharelado, Universidade Federal do Maranhão, 65085-580 São Luís, Maranhão, Brazil*

(Dated: July 7, 2026)

Standard Pancharatnam–Berry and linear-birefringent media convert optical spin into orbital angular momentum (OAM) through an anisotropy *director*, a rank-two, headless field, and therefore obey the selection rule $\Delta\ell = 2q$ per unit texture charge q . We show that a medium with geometric *torsion*, the continuum limit of a screw-dislocation array, can convert spin to OAM through the *contortion* of its material connection, which enters the effective paraxial dynamics as a rank-one vector field. The resulting selection rule is $\Delta\ell = q$. Its winding is fixed by geometry and symmetry, not by a Pancharatnam–Berry director, and the process conserves the screw charge $\tilde{J}_z = L_z + (q/2)\sigma_z$ while exchanging $(2 - q)\hbar$ of angular momentum per converted photon with the defect lattice. Paraxial simulations confirm the rule: a circular Gaussian input develops a stable, topologically quantized $\ell = +q$ vortex in the reversed helicity, with 83% conversion over three Rayleigh ranges and no fine-tuning. We propose a polarization-resolved photonic-lattice discriminator in which the slope of the measured OAM versus the independently written texture charge, one for torsion, two for birefringence, separates the two mechanisms.

Introduction. The interconversion of the spin and orbital angular momentum (OAM) of light [1–6] is the working principle of a wide class of structured-light devices. More broadly, the OAM spectrum provides an infinite-dimensional photonic degree of freedom that can be engineered for multidimensional angular-momentum states and used as a spiral spectrum to probe phase, amplitude, and dislocation features of matter [7, 8]. Its paradigm is the q -plate: an anisotropic element whose optical axis winds q times around a central defect and which flips the helicity of a photon while imprinting an OAM jump $\Delta\ell = 2q$ [9–13], a rule that carries over to dielectric metasurfaces [14] and, more generally, to any medium whose spin–orbit coupling is mediated by linear birefringence. The factor of two is not accidental: the local optic axis is a *director*, a headless, rank-two object, so its optical response winds twice per turn of the texture. This rank-two rule underlies the standard Pancharatnam–Berry route to spin-to-OAM conversion.

Here we identify a physically distinct class of converters that does not. In the geometric theory of defects [15–18], a continuous distribution of parallel screw dislocations is described by a Riemann–Cartan geometry with *torsion*: curvature-free, but with a nontrivial translational holonomy. Light in such media acquires quantized OAM modes [19], dislocation-induced anisotropy that alters its spin [20], a purely geometric optical activity linear in the dislocation density [21, 22], and torsion-controlled guidance [23]; torsion-stress-induced vortices have been observed in bulk crystals [24, 25], and photonic lattices emulating dislocated backgrounds bind vortex light [26]. We show that the object mediating spin–orbit conversion in a torsional medium is the transverse part of the *contortion* tensor, a rank-one (vector) field, that winds

once per turn of the defect texture. The selection rule is therefore

$$\Delta\ell_{\text{torsional}} = q, \quad \Delta\ell_{\text{PB}} = 2q, \quad (1)$$

per converted photon (Fig. 1). The slope of the measured OAM versus texture charge is thus a clean, binary discriminator between geometric (torsional) and birefringent conversion, a testable prediction that we quantify below for existing photonic platforms.

Model. We describe a monochromatic paraxial beam by the circular-polarization spinor $\Psi = (E_+, E_-)^T$ propagating along the defect axis z of a screw-dislocation continuum,

$$i \partial_z \Psi = \left[-\frac{1}{2k_0} \nabla_{\perp}^2 + \Gamma(r) \sigma_z + \kappa(r) \hat{\mathbf{w}} \cdot \boldsymbol{\sigma}_{\perp} \right] \Psi, \quad (2)$$

with $\hat{\mathbf{w}} \cdot \boldsymbol{\sigma}_{\perp} = \cos(q\varphi)\sigma_x + \sin(q\varphi)\sigma_y$, $k_0 = kw_0$, and transverse lengths in units of the input waist w_0 . Equation (2) is an effective paraxial Maxwell model for a structured medium; it is not an assumption of a universal vacuum coupling of photons to spacetime torsion. The material response projects two independent components of the contortion one-form of the dislocated medium, computed in the Supplemental Material (SM) [27], onto the circular-polarization subspace: the component along e^z rotates the transverse frame and gives the diagonal torsional phase rate $\Gamma(r) \propto A'(r)$, reproducing the geometric optical activity law of the uniform-torsion medium [21]; the transverse components form the contortion vector $\mathbf{w} = \frac{\tau}{2}\hat{\boldsymbol{\varphi}}$, where τ is the torsion density. The tangential direction differs from the convention used in Eq. (2) only by a constant $\pi/2$ phase, which can be absorbed into the circular-spin basis and does not affect the winding or the selection rule. The azimuthal winding is exactly $q = 1$ for the axisymmetric screw continuum and q for engineered Burgers textures of integer charge q . Because \mathbf{w} is a vector, the symmetry-allowed local Hermitian coupling that is first order in the contortion

* Edilberto O. Silva - edilberto.silva@ufma.br

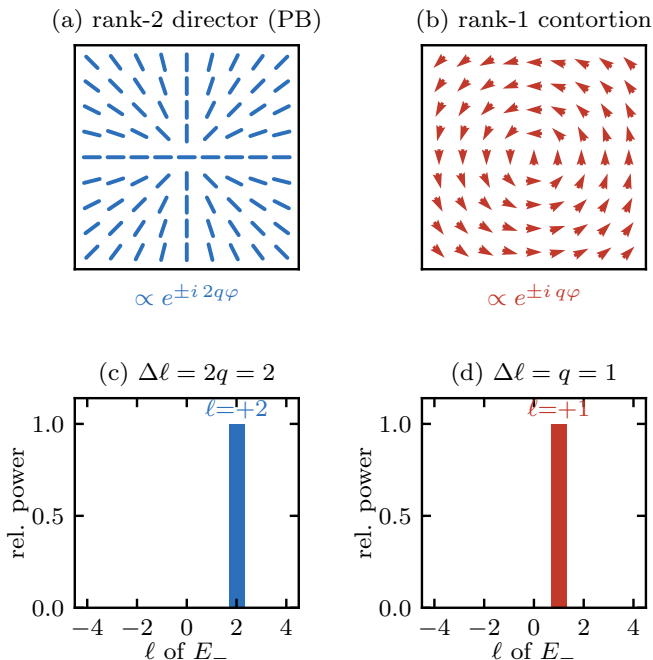


FIG. 1. The selection rule distinguishes the rank of the mediating field. (a) A Pancharatnam–Berry element couples the circular components through a rank-two director texture of charge q ; the coupling winds as $e^{\pm i2q\varphi}$. (b) A torsional (Riemann–Cartan) medium couples them through the rank-one contortion vector, which winds as $e^{\pm iq\varphi}$. (c),(d) Simulated OAM spectra of the converted beam E_- for the same texture charge $q = 1$ and identical coupling magnitude: the sideband appears at $\ell = +2$ (PB) versus $\ell = +1$ (torsional).

carries the phase $e^{\pm iq\varphi}$ in Eq. (2); rank-two combinations $w_i w_j - \frac{1}{2} \delta_{ij} \mathbf{w}^2$ wind as $e^{\pm i2q\varphi}$ and reproduce the director-mediated PB coupling instead. The holonomy amplitude $\kappa(r)$ vanishes on axis, as required by regularity, and saturates over a scale R_H ; its magnitude is not universal, but is set by the torsion density and by the magnetoelectric/elasto-optic response of the host [20, 22] (SM [27]).

The off-diagonal term feeds E_- from E_+ with the factor $e^{\pm iq\varphi}$: an input $E_+ \propto e^{im\varphi}$ generates $E_- \propto e^{i(m+q)\varphi}$, which is Eq. (1). The rule is protected by symmetry. The generator of Eq. (2) commutes with the *screw charge*

$$\tilde{J}_z = L_z + \frac{q}{2} \sigma_z, \quad L_z = -i\partial_\varphi, \quad (3)$$

the exact conserved quantity of the torsional medium; input ($\sigma_z = +1, \ell = 0$) and converted ($\sigma_z = -1, \ell = q$) states both carry $\tilde{J}_z = q/2$. The *optical* angular momentum is not conserved: each converted photon loses $2\hbar$ of spin and gains only $q\hbar$ of OAM, the balance $(2 - q)\hbar$ being exchanged as a mechanical torque with the dislocation lattice, the torsional analogue of the angular-momentum exchange in a q -plate, for which only $q = 1$ is conserving [11, 12]. Here the conserving texture is instead $q = 2$, a second, independent signature of the rank-one mechanism.

Vortex generation. We integrate Eq. (2) with a symmetric split-step scheme (parameters and convergence tests in SM [27]; baseline $k_0 = 8, \Gamma_0 = 0.8, \kappa_0 = 0.73, q = 1$, propagation to $z = 25 w_0 \approx 3z_R$). A circularly polarized Gaussian ($\ell = 0$) develops, in the reversed helicity, a phase singularity that nucleates on axis within a fraction of a Rayleigh range and locks to topological charge $n = +1$ [Fig. 2(a)]. The conversion is quantitative: the power fraction in the reversed helicity and the mean OAM grow together and saturate at $\eta = P_- \simeq 0.83, \langle L_z \rangle \simeq 0.83 \hbar$ [Fig. 2(b)]. Here $\langle L_z \rangle$ is normalized to the total input power; within the converted channel the mean OAM per photon is $\ell = +1$. The identity $\langle L_z \rangle / \hbar = \eta$ is therefore the macroscopic expression of the selection rule, and the OAM spectrum of E_- is a single line at $\ell = +1$ with purity above 0.999. Switching off the holonomy ($\kappa \equiv 0$) leaves the full Abelian torsional phase $\Gamma\sigma_z$ in place, yet produces *no* conversion and no vortex (SM [27]): the rank-one contortion coupling is the sole microscopic agent.

Robustness. The quantization and chirality of the output are structural, not tuned. Across more than one hundred simulations a 13-point sweep of κ_0 [Fig. 2(c)], a 9×9 landscape in (κ_0, Γ_0) , and paraxial parameters up to $k_0 = 64$ ($w_0 \approx 10\lambda$) the topological charge is $n = +1$ and the recorded azimuthal purity exceeds 0.999 in every run, while only the efficiency varies smoothly (η up to 0.86; $\Delta\eta < 0.2\%$ under doubling of grid or steps) [27]. The rule $\Delta\ell = q$ cannot be washed out by parameter drift: the off-diagonal coupling can only populate the $\ell = m + q$ channel.

Proposed experiment. Figure 3 shows a discriminator experiment built from demonstrated components. Femtosecond-written photonic lattices already emulate dislocated backgrounds and bind vortex light [26]. The required extra ingredient is a polarization-sensitive implementation in which the local waveguide anisotropy or bi-anisotropy is aligned with the transverse Burgers texture, so that the circular–polarization coupling is linear in the written contortion vector of Eq. (2); this can be implemented, for example, with elliptic femtosecond-written waveguides, controlled stress birefringence, or locally anisotropic couplers. Such laser-written platforms provide effective index contrasts $\delta n \sim 10^{-3}$. The accumulated rotation required for the 83% operating point is $\kappa_{\text{dim}} L \approx 18$, i.e., $L \approx 4.6$ mm at $\lambda = 800$ nm for $\delta n = 10^{-3}$, a centimeter-class chip; twisted photonic-crystal fibers [28] and liquid-crystal realizations of dislocated media [19] give $\delta n \sim 10^{-4}$ and centimeter lengths. A σ^+ Gaussian is launched along the defect axis; the output is helicity-sorted (quarter-wave plate and polarizing splitter) and the OAM content of the reversed-helicity channel is read out by a mode sorter or tilted-lens diagnostics. The smoking gun is the slope of the measured ℓ versus the independently written texture charge q [Fig. 3(b)]: unity for the torsional mechanism, two for a birefringence-mediated (PB) response. Although PB plates may employ half-integer director charges, the pro-

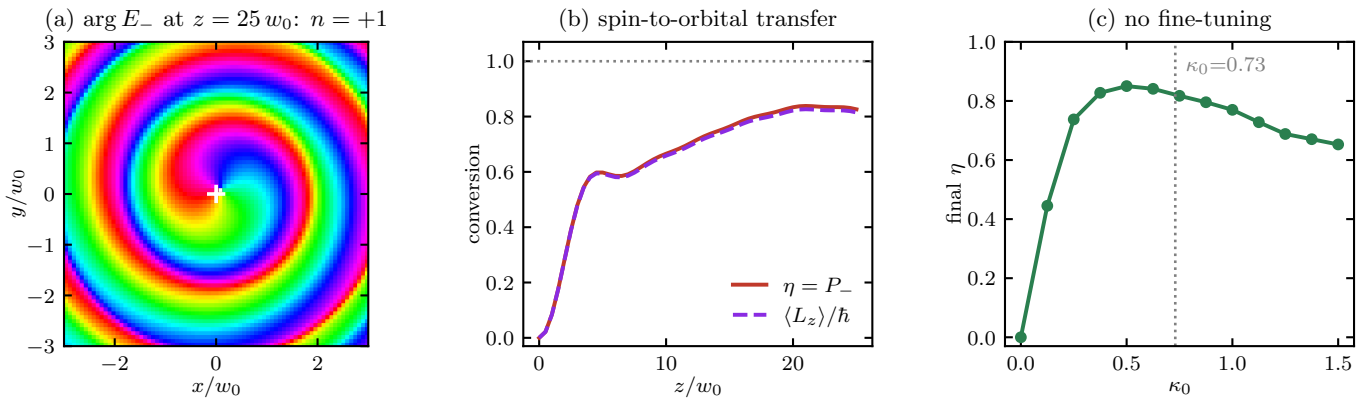


FIG. 2. Torsional vortex generation ($q = 1$). (a) Phase of the converted field at $z = 25 w_0$: a stable, charge- $n=+1$ spiral. (b) Conversion $\eta = P_-$ and mean OAM versus propagation distance; both saturate at 0.83. (c) Final conversion versus holonomy strength κ_0 : a broad maximum ($\eta \simeq 0.85$) with no fine-tuning; in every run the charge is quantized at $n = +1$. Full sweeps in (κ_0, Γ_0) , paraxial parameter $k_0 = 8\text{--}64$, and grid refinement are given in the SM [27].

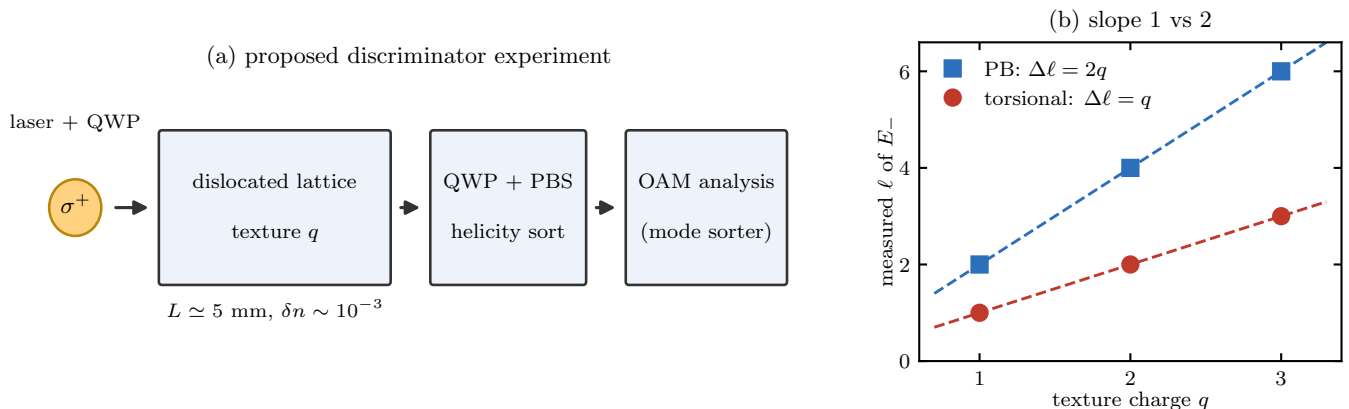


FIG. 3. Proposed discriminator. (a) A circularly polarized Gaussian traverses a femtosecond-written lattice with a screw-dislocation texture of charge q ($L \simeq 5 \text{ mm}$ at $\delta n \sim 10^{-3}$); the output is helicity-sorted and its OAM measured. (b) Predicted OAM of the converted beam versus texture charge, from full simulations of Eq. (2) (circles) and of a PB-type rank-two coupling of identical magnitude (squares): slopes 1 and 2, with no overlap at any integer q .

posed test compares devices with the same integer vector texture q , for which the $\ell = q$ and $\ell = 2q$ sidebands do not overlap. Reversing either the input helicity or the sign of the Burgers texture must reverse the sideband, $\ell \rightarrow -\ell$, providing an additional control against residual PB leakage. Two corroborating signatures come for free: for $q = 2$ the torsional conversion is angular-momentum conserving, so no torque is exerted on the lattice, whereas the PB response at $q = 2$ requires an equal-and-opposite exchange of $2\hbar$ per converted photon with the medium; and the converted power follows the distributed (Rabi-like) growth of Fig. 2(b) rather than the thin-element retardation law of a q -plate.

Discussion. Equation (1) elevates the OAM jump per unit texture charge to a measurement of the *rank* of the geometric object that couples light's spin to its spatial structure: directors give two, vectors give one. Torsion provides the natural physical realization of the rank-one case: the contortion of a Riemann–Cartan medium is

a transverse vector field whose winding is fixed by the defect topology, not by a material director. The associated conserved charge (3), the mechanical torque $(2-q)\hbar$ per converted photon, and the distributed conversion dynamics complete a phenomenology that is qualitatively distinct from the Pancharatnam–Berry paradigm. Beyond structured light, the effect gives photonics a direct probe of material torsion: the conversion efficiency and sideband position measure the dislocation density and texture charge of the medium, complementing recent proposals for torsion metrology in electronic systems [29, 30] and extending the toolbox of geometric and topological photonics [31–35] to non-Riemannian backgrounds.

ACKNOWLEDGMENTS

The author thanks Lluís Torner for stimulating correspondence on the inverse characterization of torsional

optical media from spiral spectra. This work was supported by CAPES (Finance Code 001), CNPq (Grant

306308/2022-3), and FAPEMA (Grants UNIVERSAL-06395/22 and APP-12256/22).

-
- [1] L. Allen, M. W. Beijersbergen, R. J. C. Spreeuw, and J. P. Woerdman, *Phys. Rev. A* **45**, 8185 (1992).
- [2] V. S. Liberman and B. Y. Zel'dovich, *Phys. Rev. A* **46**, 5199 (1992).
- [3] K. Y. Bliokh, A. Niv, V. Kleiner, and E. Hasman, *Nat. Photon.* **2**, 748 (2008).
- [4] K. Y. Bliokh, F. J. Rodríguez-Fortuño, F. Nori, and A. V. Zayats, *Nat. Photon.* **9**, 796 (2015).
- [5] Y. Shen, X. Wang, Z. Xie, C. Min, X. Fu, Q. Liu, M. Gong, and X. Yuan, *Light Sci. Appl.* **8**, 90 (2019).
- [6] A. Forbes, M. de Oliveira, and M. R. Dennis, *Nat. Photon.* **15**, 253 (2021).
- [7] G. Molina-Terriza, J. P. Torres, and L. Torner, *Physical Review Letters* **88**, 013601 (2002).
- [8] L. Torner, J. P. Torres, and S. Carrasco, *Optics Express* **13**, 873 (2005).
- [9] S. Pancharatnam, *Proc. Indian Acad. Sci. A* **44**, 247 (1956).
- [10] M. V. Berry, *Proc. R. Soc. London A* **392**, 45 (1984).
- [11] L. Marrucci, C. Manzo, and D. Paparo, *Phys. Rev. Lett.* **96**, 163905 (2006).
- [12] L. Marrucci, E. Karimi, S. Slussarenko, B. Piccirillo, E. Santamato, E. Nagali, and F. Sciarrino, *J. Opt.* **13**, 064001 (2011).
- [13] A. Rubano, F. Cardano, B. Piccirillo, and L. Marrucci, *J. Opt. Soc. Am. B* **36**, D70 (2019).
- [14] R. C. Devlin, A. Ambrosio, N. A. Rubin, J. P. B. Mueller, and F. Capasso, *Science* **358**, 896 (2017).
- [15] B. A. Bilby, R. Bullough, and E. Smith, *Proc. R. Soc. London A* **231**, 263 (1955).
- [16] E. Kröner, *Appl. Mech. Rev.* **15**, 599 (1962).
- [17] M. O. Katanaev and I. V. Volovich, *Ann. Phys. (N.Y.)* **216**, 1 (1992).
- [18] R. A. Puntigam and H. H. Soleng, *Class. Quantum Grav.* **14**, 1129 (1997).
- [19] S. Fumeron, E. Pereira, and F. Moraes, *Physica B* **476**, 19 (2015).
- [20] L. Mashhadi and M. Mehrafarin, *J. Opt.* **12**, 035703 (2010).
- [21] H. Belich and E. O. Silva, *Geometrical optical activity induced by a continuous distribution of screw dislocations*, arXiv:2601.10841 (2026), arXiv:2601.10841.
- [22] Y.-L. Zhang, L.-N. Shi, X.-Z. Dong, F.-Z. Gong, Z.-S. Zhao, and X.-M. Duan, *On the geometry and topology of transformation optics*, arXiv:1301.6954 (2014), arXiv:1301.6954.
- [23] S. Gurtas Dogan, O. Mustafa, A. Guvendi, and H. Hasanabadi, *Eur. Phys. J. C* **86**, 31 (2026).
- [24] I. Skab, Y. Vasyukiv, V. Savaryn, and R. Vlokh, *J. Opt. Soc. Am. A* **28**, 633 (2011).
- [25] Y. Vasyukiv, O. Kvasnyuk, Y. Shopa, and R. Vlokh, *Journal of the Optical Society of America A* **30**, 891 (2013).
- [26] C. Sheng, Y. Wang, Y. Chang, H. Wang, Y. Lu, Y. Yang, S. Zhu, X. Jin, and H. Liu, *Light Sci. Appl.* **11**, 243 (2022).
- [27] See Supplemental Material included with this arXiv submission.
- [28] P. S. J. Russell, R. Beravat, and G. K. L. Wong, *Philos. Trans. R. Soc. A* **375**, 20150440 (2017).
- [29] E. O. Silva, *Ann. Phys. (Berlin)*, 2500593 (2026).
- [30] A. S. Baimuratov, I. D. Rukhlenko, R. E. Noskov, P. Ginzburg, Y. K. Gun'ko, A. V. Baranov, and A. V. Fedorov, *Sci. Rep.* **5**, 14712 (2015).
- [31] J. B. Pendry, D. Schurig, and D. R. Smith, *Science* **312**, 1780 (2006).
- [32] U. Leonhardt and T. G. Philbin, *New J. Phys.* **8**, 247 (2006).
- [33] C. Sheng, H. Liu, Y. Wang, S. N. Zhu, and D. A. Genov, *Nature Photonics* **7**, 902 (2013).
- [34] R. Bekenstein, R. Schley, M. Mutzafi, C. Rotschild, and M. Segev, *Nat. Phys.* **11**, 872 (2015).
- [35] T. Ozawa *et al.*, *Rev. Mod. Phys.* **91**, 015006 (2019).